Proceedings of the 17th World Congress
The International Federation of Automatic Control
Seoul, Korea, July 6-11, 2008

Position and Velocity Navigation Filters for Marine Vehicles

Pedro Batista [2] **Carlos Silvestre Paulo Oliveira**

Instituto Superior Técnico and Institute for Systems and Robotics
Av. Rovisco Pais, 1049-001 Lisboa, Portugal
{pbatista,cjs,pjcro}@isr.ist.utl.pt

Abstract: This paper presents the design and performance evaluation of two globally stable time varying kinematic Navigation Kalman filters to estimate linear motion quantities, in three dimensions, with application to underwater vehicles. The proposed technique is based on the linear time invariant Kalman filter steady state solution and employs frequency weights to explicitly achieve adequate wave disturbance rejection and attenuation of the noise of the sensors on the state estimates. In the first case study a Navigation filter is designed for the estimation of unknown constant ocean currents, linear position, and inertial velocity of an underwater vehicle with respect to a fixed point in the mission scenario. In the second case the proposed solution also addresses the estimation of the acceleration of gravity. The theoretical background is briefly introduced and simulation results are offered that illustrate the achievable performance in the presence of extreme environmental disturbances and realistic noise of the sensors.

1. INTRODUCTION

The design of Navigation and Positioning Systems plays a key role in the development of a large variety of mobile platforms for land, air, space, and marine applications. In the domain of marine research, the quality of the Navigation data is a fundamental requirement in applications that range from ocean sonar surveying to ocean data acquisition (salinity, temperature, etc) or sample collection (microbial organisms, sediments, etc), as the acquired data sets should be properly georeferenced with respect to a given mission reference point. For control purposes other quantities such as the attitude of the vehicle and/or the linear and angular velocities are also commonly required.

This paper presents the design and performance evaluation of globally stable time varying kinematic Navigation Kalman filters to estimate linear motion quantities, in three dimensions, with application to underwater vehicles. Related work can be found in Fossen and Strand (1999) where a globally exponentially stable (GES) observer for ships (in two-dimensions) that includes features such as wave filtering and bias estimation is presented and in H. Nijmeijer and T. I. Fossen (Eds) (1999) an extension to this result with adaptive wave filtering is available. An alternative filter was proposed in Pascoal et al. (2000) where the problem of estimating the velocity and position of an autonomous vehicle in three-dimensions was solved resorting to special bilinear time-varying complementary filters. In Refsnes et al. (2006) a pair of coworking GES observers for underwater vehicles is presented that includes the ocean current in the plant model to improve the performance of the observer. A passivity based controller-observer design for robots with n degrees of freedom is proposed in Berghuis and Nijmeijer (1993) and a sliding mode observer for robotic manipulators is reported in C. De Wit and J.-J. Slotine (1991). The development of nonlinear observers for Euler-Lagrange systems has been addressed in Skjetne and Shim (2001) and Ortega et al. (1998). In these approaches robustness to environmental disturbances and/or noise of the sensors is considered but no optimal results are provided.

The methodology proposed in this paper relies on the design and implementation of optimal time-varying Navigation filters based on the steady state Kalman filter solution for equivalent linear time invariant (LTI) systems. Furthermore, the design methodology permits the use of frequency weights to explicitly achieve adequate wave disturbance rejection and attenuation of the noise of the sensors on the state estimates. Two case studies are presented: *i)* in the first one a filter is designed for the estimation of unknown constant ocean currents, linear position, and inertial velocity of an underwater vehicle with respect to a fixed point in the mission scenario; *ii)* in the second one the proposed filter also addresses the estimation of the acceleration of gravity.

The paper is organized as follows. The theoretical results behind the proposed solutions are summarized in Section 2. In Section 3 the first case study is presented for the estimation of the position and velocity of an underwater vehicle and the velocity of constant ocean currents. Sim-

[1] This work was partially supported by Fundação para a Ciência e a Tecnologia (ISR/IST plurianual funding) and project MEDIRES from ADI through the POS_Conhecimento Program that includes FEDER funds, and by the project PDCT/MAR/55609/2004 - RUMOS of the FCT.
[2] The work of P. Batista was supported by a PhD Student Scholarship from the POCTI Programme of FCT, SFRH/BD/24862/2005.

978-1-1234-7890-2/08/$20.00 © 2008 IFAC **10.3182/20080706-5-KR-1001.1947**

ulation results are offered that illustrate the achievable performance in the presence of extreme environmental disturbances and realistic noise of the sensors. The second estimation solution, which also deals with the estimation of the gravity acceleration, is presented in Section 4. Simulation results are also offered to evaluate the resulting performance. Finally, Section 5 summarizes the main contributions of the paper.

Throughout the paper the symbol $\mathbf{0}_{n\times m}$ denotes an $n \times m$ matrix of zeros, $\mathbf{I}_n$ an identity matrix with dimension $n \times n$, and $\mathrm{diag}(\mathbf{A}_1, \ldots, \mathbf{A}_\mathrm{n})$ a block diagonal matrix. When the dimensions are omitted the matrices are assumed of appropriate dimensions.

2. THEORETICAL BACKGROUND

This section briefly introduces the kinematic filter design methodology adopted in the present work, for further details the reader is referred to Batista et al. (2008). The solution relies on the design of optimal time-varying filters based on the steady state Kalman filter for equivalent linear time invariant systems. This is achieved through the use of an orthogonal Lyapunov transformation and frequency weights may be employed to explicitly attain adequate wave disturbance rejection and attenuation of the noise of the sensors on the state estimates.

Consider the class of dynamic systems

$$\begin{cases} \dot{\boldsymbol{\eta}}_p(t) = \mathbf{A}_p \boldsymbol{\eta}_p(t) - \mathbf{M}_S\left(\boldsymbol{\omega}(t)\right)\boldsymbol{\eta}_p(t) + \mathbf{B}_p(t)\mathbf{u}(t) + \mathbf{T}^T(t)\mathbf{L}_p\mathbf{d}(t) \\ \boldsymbol{\psi}(t) = \boldsymbol{C}_p\boldsymbol{\eta}_p(t) + \mathbf{R}^T(t)\mathbf{M}_p\mathbf{n}(t) \end{cases}, \tag{1}$$

where

- $\boldsymbol{\eta}_p(t) = \left[\boldsymbol{\eta}_1^T(t) \ldots \boldsymbol{\eta}_N^T(t)\right]^T$, with $\boldsymbol{\eta}_i(t) \in X_i \subseteq \mathbb{R}^3$, $i = 1, \ldots, N$, is the system state,
- $\boldsymbol{\psi}(t) \in \mathbb{R}^3$ is the system output,
- $\mathbf{u}(t)$ is a deterministic system input,
- $\boldsymbol{\omega}(t) \in \mathbb{R}^3$ is a continuous bounded function of t,
- $\mathbf{d}(t)$ denotes the system disturbances input,
- $\mathbf{n}(t)$ denotes the noise of the sensors,
- $\mathbf{M}_S\left(\boldsymbol{\omega}(t)\right)$ is the block diagonal matrix
$$\mathbf{M}_S\left(\boldsymbol{\omega}(t)\right) := \mathrm{diag}\left(\mathbf{S}(\boldsymbol{\omega}(t)), \ldots, \mathbf{S}(\boldsymbol{\omega}(t))\right),$$
where $\mathbf{S}(\boldsymbol{\omega}(t))$ is a skew-symmetric matrix that verifies $\mathbf{S}\left(\mathbf{a}\right)\mathbf{b} = \mathbf{a} \times \mathbf{b}$, with $\times$ denoting the cross product, and that satisfies
$$\dot{\mathbf{R}}(t) = \mathbf{R}(t)\mathbf{S}(\boldsymbol{\omega}(t)),$$
where $\mathbf{R}(t) \in \left\{\mathbf{R} \in \mathbb{R}^{3\times 3} : \mathbf{R}\mathbf{R}^T = \mathbf{I}_3,\ \det(\mathbf{R}) = 1\right\}$, i.e., $\mathbf{R}(t)$ is a proper rotation matrix,
- $$\mathbf{A}_p = \begin{bmatrix} \mathbf{0} & \gamma_1\mathbf{I} & \mathbf{0} & \ldots & \mathbf{0} \\ \vdots & \ddots & \ddots & \ddots & \vdots \\ \vdots & & \ddots & \ddots & \mathbf{0} \\ \vdots & & & \ddots & \gamma_{N-1}\mathbf{I} \\ \mathbf{0} & \ldots & \ldots & \ldots & \mathbf{0} \end{bmatrix},$$
where $\gamma_i \in \mathbb{R}$, $\gamma_i \neq 0$, $i = 1, \ldots, N-1$,
- $\mathbf{C}_p = [\mathbf{I}_3\ \mathbf{0}_{3\times 3} \ldots \mathbf{0}_{3\times 3}]$, and
- $\mathbf{T}(t) := \mathrm{diag}\left(\mathbf{R}(\mathrm{t}), \ldots, \mathbf{R}(\mathrm{t})\right)$.

It is assumed that $\mathbf{M}_p$ is a full row-rank matrix and $\mathbf{R}(t)$ and $\boldsymbol{\omega}(t)$ are known over time. Notice that the disturbance input $\mathbf{d}$ and the noise of the sensors $\mathbf{n}$ affect the state and the system output through time varying rotation transformations, $\mathbf{T}(t)$ and $\mathbf{R}(t)$, respectively. Nevertheless, these transformations preserve the norm of the disturbances and the noise of the sensors - only the directionality is affected over time.

For design purposes, consider the augmented plant as depicted in Fig. 1. In the figure $\mathbf{w}_1$ and $\mathbf{w}_2$ represent generalized disturbance vectors and $\mathcal{W}_d$ and $\mathcal{W}_n$ are linear time invariant filters included to shape both the noise of the sensors $\mathbf{n}$ and the state disturbances $\mathbf{d}$.

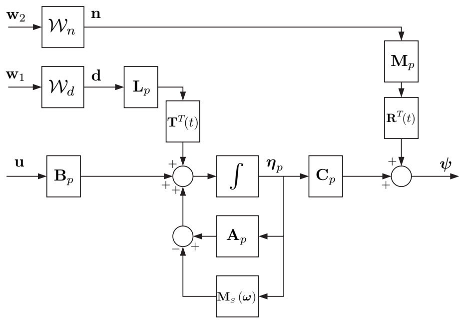

Fig. 1. Generalized design framework

Let $\mathbf{w}(t) := \left[\mathbf{w}_1^T(t)\, \mathbf{w}_2^T(t)\right]^T$ and define the augmented state vector $\boldsymbol{\eta}(t) := \left[\boldsymbol{\eta}_p^T(t)\, \mathbf{x}_d^T(t)\, \mathbf{x}_n^T(t)\right]^T$, where $\mathbf{x}_d$ and $\mathbf{x}_n$ denote the states of the state space realizations $(\mathbf{A}_d, \mathbf{B}_d, \mathbf{C}_d, \mathbf{D}_d)$ and $(\mathbf{A}_n, \mathbf{B}_n, \mathbf{C}_n, \mathbf{D}_n)$ of the filters $\mathcal{W}_d$ and $\mathcal{W}_n$, respectively. The augmented dynamics corresponding to the generalized design framework, depicted in Fig. 1, can be written as

$$\begin{cases} \dot{\boldsymbol{\eta}}(t) = \boldsymbol{\mathcal{A}}(t)\boldsymbol{\eta}(t) + \boldsymbol{\mathcal{B}}_p(t)\mathbf{u}(t) + \boldsymbol{\mathcal{B}}(t)\mathbf{w}(t) \\ \boldsymbol{\psi}(t) = \boldsymbol{\mathcal{C}}(t)\boldsymbol{\eta}(t) + \boldsymbol{\mathcal{D}}(t)\mathbf{w}(t) \end{cases},$$

where the definition of the various matrices is omitted since it is evident from the context. Before presenting the main result of this section the following definitions are required. Let

$$\mathbf{A} := \begin{bmatrix} \mathbf{A}_p & \mathbf{L}_p\mathbf{C}_d & \mathbf{0} \\ \mathbf{0} & \mathbf{A}_d & \mathbf{0} \\ \mathbf{0} & \mathbf{0} & \mathbf{A}_n \end{bmatrix}, \quad \mathbf{B} := \begin{bmatrix} \mathbf{L}_p\mathbf{D}_d & 0 \\ \mathbf{B}_d & \mathbf{0} \\ \mathbf{0} & \mathbf{B}_n \end{bmatrix},$$

$\mathbf{C} := [\mathbf{C}_p\ \mathbf{0}\ \mathbf{M}_p\mathbf{C}_n]$, and $\mathbf{D} := [\mathbf{0}\ \mathbf{M}_p\mathbf{D}_n]$. Define also

$$\mathbf{V} := \begin{bmatrix} \mathbf{B} \\ \mathbf{D} \end{bmatrix} \begin{bmatrix} \mathbf{B}^T\, \mathbf{D}^T \end{bmatrix} = \begin{bmatrix} \mathbf{V}_{xx} & \mathbf{V}_{xy} \\ \mathbf{V}_{xy}^T & \mathbf{V}_{yy} \end{bmatrix}.$$

The following theorem presents the optimal Kalman filter for the class of systems (1).

Theorem 1. Consider the generalized system dynamics as depicted in Fig. (1), where $\mathbf{w}$ is assumed to be continuous-time zero-mean unit intensity white noise. Let $\boldsymbol{\mathcal{P}}_0$ be the initial covariance matrix of the augmented system state $\boldsymbol{\eta}$. Then, the optimal Kalman filter is given by

$$\begin{cases} \dot{\hat{\boldsymbol{\eta}}}(t) = \boldsymbol{\mathcal{A}}(t)\hat{\boldsymbol{\eta}}(t) + \boldsymbol{\mathcal{B}}_p(t)\mathbf{u}(t) + \boldsymbol{\mathcal{K}}_2(t)\left[\boldsymbol{\psi}(t) - \boldsymbol{\mathcal{C}}(t)\hat{\boldsymbol{\eta}}(t)\right] \\ \hat{\boldsymbol{\psi}}(t) = \boldsymbol{\mathcal{C}}(t)\hat{\boldsymbol{\eta}}(t) \end{cases},$$

where $\boldsymbol{\mathcal{K}}_2(t) := \mathbf{T}_c^T(t)\mathbf{K}_2(t)\mathbf{R}(t)$, with

$$\mathbf{K}_2(t) := \left[\mathbf{P}_2(t)\mathbf{C}^T + \mathbf{V}_{xy}\right]\mathbf{V}_{yy}^{-1},$$

$$\mathbf{T}_c(t) := \operatorname{diag}\left(\mathbf{T}(\mathrm{t}), \mathbf{I}, \mathbf{I}\right),$$

and $\mathbf{P}_2(t)$ is the solution of the differential matrix Riccati equation

$$\dot{\mathbf{P}}_2(t) = \mathbf{A}_e\mathbf{P}_2(t) + \mathbf{P}_2(t)\mathbf{A}_e^T - \mathbf{P}_2(t)\mathbf{C}^T\mathbf{V}_{yy}^{-1}\mathbf{C}\mathbf{P}_2(t) + \mathbf{V}_{xx} - \mathbf{V}_{xy}\mathbf{V}_{yy}^{-1}\mathbf{V}_{xy}^T, \quad (2)$$

with $\mathbf{P}_2(t_0) = \mathbf{T}_c\left(t_0\right)\boldsymbol{\mathcal{P}}_0\mathbf{T}_c^T(t_0)$ and $\mathbf{A}_e := \mathbf{A} - \mathbf{V}_{xy}\mathbf{V}_{yy}^{-1}\mathbf{C}$.

Proof. The proof, which relies on the transformation of the linear time varying (LTV) system into an LTI system, is omitted here due to the lack of space but can be found in Batista et al. (2008).

Notice that the proposed Kalman filter gain matrix $\boldsymbol{\mathcal{K}}_2(t)$ has a limit solution, although the system at hand is not LTI. Indeed, as t approaches infinity, $\mathbf{P}_2(t)$ converges to the solution $\mathbf{P}_2^\infty$ of the matrix Riccati equation

$$\mathbf{A}_e\mathbf{P}_2^\infty + \mathbf{P}_2^\infty\mathbf{A}_e^T - \mathbf{P}_2^\infty\mathbf{C}^T\mathbf{V}_{yy}^{-1}\mathbf{C}\mathbf{P}_2^\infty + \mathbf{V}_{xx} - \mathbf{V}_{xy}\mathbf{V}_{yy}^{-1}\mathbf{V}_{xy}^T = \mathbf{0}.$$

Thus, as t approaches infinity, $\mathbf{K}_2$ converges to $\mathbf{K}_2^\infty := \left[\mathbf{P}_2^\infty\mathbf{C}^T + \mathbf{V}_{xy}\right]\mathbf{V}_{yy}^{-1}$ and the filter gain to

$$\lim_{t\to\infty}\boldsymbol{\mathcal{K}}_2(t) = \mathbf{T}_c^T(t)\mathbf{K}_2^\infty\mathbf{R}(t).$$

This is a fundamental property in practical applications, as the filter gain can be replaced by the corresponding limit solution, $\mathbf{T}_c^T(t)\mathbf{K}_2^\infty\mathbf{R}(t)$, of which $\mathbf{K}_2^\infty$ can be easily obtained offline from the solution of an algebraic Riccati equation.

3. POSITION AND CURRENT ESTIMATION

3.1 Problem Statement

The example provided in this section revisits the problem first described in Batista et al. (2006). Consider an underwater vehicle equipped with an acoustic positioning system like an Ultra Short Base Line (USBL) sensor and suppose that there is a moored buoy in the mission scenario where an acoustic transponder is installed. The linear motion kinematics of the vehicle can be written as

$$\dot{\mathbf{p}} = \mathbf{R}\mathbf{v}, \quad (3)$$

where $\mathbf{p}$ is the position of the origin of the body-fixed coordinate system $\{B\}$ described in the inertial coordinate system $\{I\}$, $\mathbf{R}$ is the rotation matrix from $\{B\}$ to $\{I\}$, that verifies $\dot{\mathbf{R}} = \mathbf{R}\mathbf{S}(\boldsymbol{\omega})$, $\mathbf{v}$ is the linear velocity of the vehicle relative to $\{I\}$, expressed in body-fixed coordinates, and $\boldsymbol{\omega}$ is the vehicle angular velocity, also expressed in body-fixed coordinates. Assume that the buoy where the transponder is installed is subject to wave action of known power spectral density that affects its position over time, and suppose that the position of the vehicle with respect to the transponder is available, in body-fixed coordinates as measured by the USBL sensor installed on-board. Suppose also that the body angular velocity $\boldsymbol{\omega}$ and the rotation matrix $\mathbf{R}$ are available from an Attitude and Heading Reference System (AHRS). Finally, suppose that the vehicle is moving in deep waters (far from the wave action), in the presence of an ocean current of constant velocity, which expressed in body-fixed coordinates is represented by $\mathbf{v}_c$.

The problem considered here is that of estimate the velocity of the current and the position of the vehicle with respect to the transponder. Further consider that the velocity of the vehicle relative to the water is available from the measures of an on-board Doppler velocity log. In shallow waters, this sensor can be employed to measure both the velocity of the vehicle relative to the inertial frame and relative to the water. However, when the vehicle is far from the bottom the inertial velocity is usually unavailable. By estimating the ocean current velocity, an estimate of the velocity of the vehicle relative to the inertial frame is immediately obtained.

3.2 Proposed Solution

Let $\mathbf{e}$ denote the position of the transponder and $\mathbf{v}_r$ denote the velocity of the vehicle relative to the fluid, both expressed in body-fixed coordinates. Since the transponder is assumed at rest (in the absence of environmental disturbances) in the inertial frame, the time derivative of $\mathbf{e}$ is given by

$$\dot{\mathbf{e}} = -\mathbf{v}_r - \mathbf{v}_c - \mathbf{S}\left(\boldsymbol{\omega}\right)\mathbf{e}. \quad (4)$$

On the other hand, since the velocity of the fluid is assumed to be constant in the inertial frame, the time derivative of this quantity expressed in body-fixed coordinates is simply given by

$$\dot{\mathbf{v}}_c = -\mathbf{S}(\boldsymbol{\omega})\mathbf{v}_c.$$

Notice that the vehicle velocity relative to the inertial frame satisfies $\mathbf{v} = \mathbf{v}_r + \mathbf{v}_c$.

Clearly, the problem of estimating the velocity of the fluid, $\mathbf{v}_c$, falls into the class of problems addressed in Section 2, with $\boldsymbol{\eta}_1 = \mathbf{e}$, $\boldsymbol{\eta}_2 = \mathbf{v}_c$,

$$\mathbf{A}_p = \begin{bmatrix} \mathbf{0} & -\mathbf{I}_3 \\ \mathbf{0} & \mathbf{0} \end{bmatrix}, \quad \mathbf{B}_p(t) = \begin{bmatrix} -\mathbf{I}_3 \\ \mathbf{0} \end{bmatrix},$$

and $\mathbf{u} = \mathbf{v}_r$. Thus, it is possible to design an optimal Kalman filter using the methodology introduced in the previous section.

Note that, in this case, the position of the transponder changes with time as the latter is assumed to be mounted in a buoy close to the sea surface, subject to strong wave action. Nevertheless, the buoy wave induced random motion can be modeled as an external disturbance on the USBL positioning system expressed on the inertial frame, and its description embedded in the frequency weights as presented in Section 2. As filter design objective consider the rejection of the wave induced disturbances from the position measurements to the position and current velocity estimates, as well as the noise in the position and relative velocity measurements.

The disturbances induced by the three-dimensional wave random field in the position of the buoy are modeled using three second-order harmonic oscillators representing the disturbance models along the x, y, and z directions,

$$H_w^i(s) = \frac{\sigma_i s}{s^2 + 2\xi_i\omega_{0i}s + \omega_{0i}^2},\ i = 1,\, 2,\, 3,$$

where ω_{0i} is the dominating wave frequency along each axis, ξ_i is the relative damping ratio, and σ_i is a parameter related to the wave intensity, see Fossen and Strand (1999) and Silvestre et al. (1997) for further details. The sensor frequency weight matrix transfer function $\mathbf{W}_n(s)$ was chosen as

$$\mathbf{W}_n(s) = \left(1 + \frac{\sigma_i s}{s^2 + 2\xi_i \omega_{0i} s + \omega_{0i}^2}\right) \mathbf{I}_3.$$

Notice that a direct term was included, not only to satisfy design requirements (nonzero sensor noise), but also to model the noise on the USBL, which was assumed Gaussian with standard deviation of 1 m. In the simulation the dominating wave frequency was set to $\omega_{0i} = 0.8975\text{rad/s}$ and the relative damping ratio to $\xi_i = 0.1$.

In addition to the disturbances induced by ocean waves and the noise on the USBL positioning system, in the simulation the measurements of the vehicle velocity relative to the water and the angular velocity were also assumed to be corrupted by Gaussian noise, with standard deviations of 0.01 m/s and 0.02 °/s, respectively. The system disturbance weight transfer matrix was chosen as $\mathbf{W}_d(s) = 0.01\mathbf{I}_6$.

Albeit it was not explicitly shown, the Kalman filter error dynamics have an equivalent LTI description, which relates to the LTV dynamics through the transformation matrix $\mathbf{T}_c(t)$, which preserves the norm of the different state estimation errors and only affects the directionality over time. Fig. 2 shows the singular values of the linear time invariant closed loop transfer functions from the disturbances and sensor noise input, $\mathbf{d}$ and $\mathbf{n}$, respectively, to the position and current velocity estimate errors, in the inertial frame, of the Kalman filter. The diagram shows that the performance requirements are met by the resultant filter, which is evident from the band rejection characteristics of the notch present in the diagram.

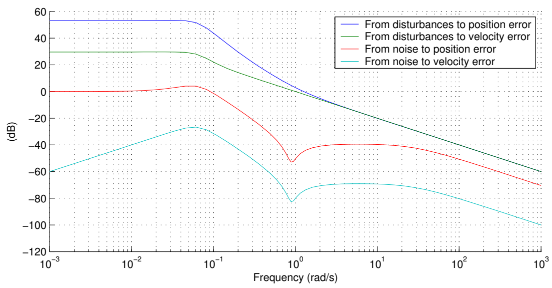

Fig. 2. Singular values of the Kalman LTI filter error dynamics

3.3 Simulation results

To illustrate the performance of the proposed solution a simulation was carried out with a simplified model of the SIRENE underwater vehicle, see Silvestre et al. (1998).

The trajectory described by the vehicle is shown in Fig. 3, where the undisturbed position of the buoy is marked with a cross and the initial position of the vehicle coincides with the origin of the inertial frame. The actual position of the buoy, expressed in inertial frame coordinates, is depicted in Fig. 4. As it can be seen, the buoy wave induced random motion is confined to an interval of about 10 m of height, which corresponds to extreme weather conditions.

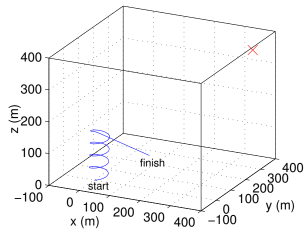

Fig. 3. Trajectory described by the vehicle

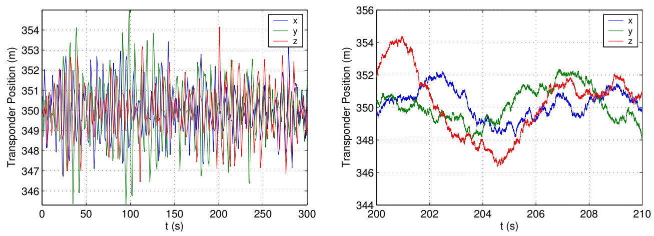

(a) Overall (b) Zoom

Fig. 4. Time evolution of the position of the buoy (expressed in inertial coordinates)

The filter initial states were chosen to reflect the knowledge of the position of the transponder as given by the USBL sensor. Fig. 5 presents the time evolution of the estimates of the Kalman filter. The position of the buoy if there were no ocean waves is also shown, as well as the actual velocity of the fluid, all expressed in body-fixed coordinates. From these plots the performance of the filter is evident - only the initial transients are noticeable.

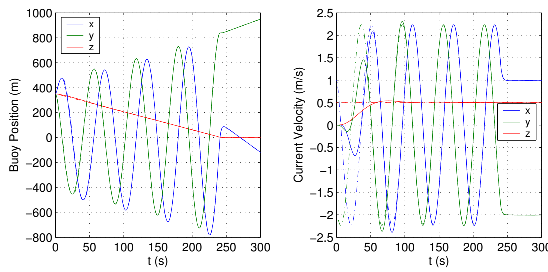

Fig. 5. Actual (dash-dot lines) and estimated (solid lines) variables

The evolution of the filter error variables is shown in Fig. 6. The initial transients arise due to the mismatch of the initial conditions of the states of the filter and can be considered as a warming up time of 180 s of the corresponding Integrated Navigation System. The filter error variables are shown in greater detail in Fig. 7. From the various plots it can be concluded that the disturbances induced by the waves, as well as the noise of the sensors, are highly attenuated by the filter, producing very accurate estimates of the velocity of the current and the position of the buoy.

Notice that if the position of the transponder at rest in the inertial frame is known to the vehicle, then an estimate of the actual position of the vehicle in the inertial frame is simply obtained from

$$\mathbf{p} = {}^{I}(\mathbf{e}) - \mathbf{R}\mathbf{e},$$

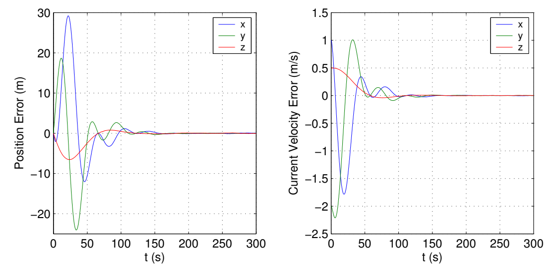

Fig. 6. Time evolution of the Kalman filter error variables

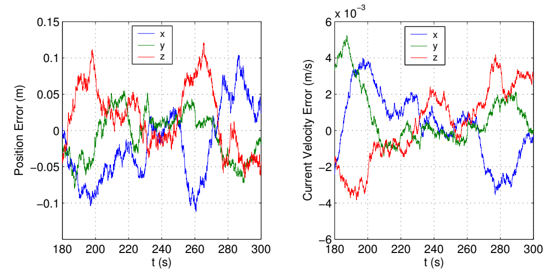

Fig. 7. Detailed evolution of the Kalman filter error variables

where ${}^{I}(\mathbf{e})$ is the position of the transponder expressed in the inertial frame. Fig. 8(a) depicts the actual and the estimated vehicle trajectories. For comparison purposes, the non-filtered position of the vehicle is plotted in Fig. 8(b). It is clear how accurate the filter estimates the trajectory described by the vehicle, even in the presence of severe wave action affecting the position of the buoy and realistic noise of the sensors.

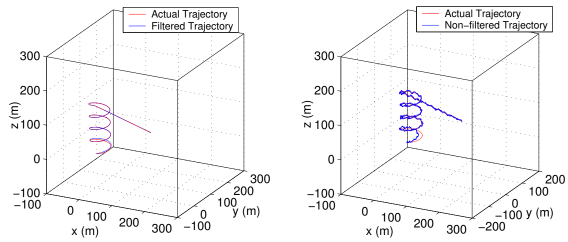

(a) Estimated trajectory (b) Non-filtered trajectory

Fig. 8. Vehicle trajectory

To conclude the discussion it should be said that the proposed solution for the estimation of the position and the velocity of the ocean current is optimal with respect to disturbances arising from all sensors but the Attitude and Heading Reference System (AHRS). Nevertheless, the performance exhibited by the proposed filter is good, as the simulation results clearly demonstrate.

4. POSITION, VELOCITY, AND GRAVITY ESTIMATION

4.1 Problem Statement

As in the previous section, consider a vehicle with kinematics (3) moving in a mission scenario where a transponder is installed, also subject to environmental disturbances of known power spectral density. Suppose that the position of the transponder is available, in body-fixed coordinates, as well as the vehicle angular velocity and the rotation matrix $\mathbf{R}$ from body-fixed coordinates to inertial coordinates. Finally, suppose that the vehicle is equipped with an accelerometer, whose measures satisfy

$$\mathbf{a} = \dot{\mathbf{v}} + \mathbf{g} + \mathbf{S}(\boldsymbol{\omega})\mathbf{v}, \tag{5}$$

where $\mathbf{a}$ is the accelerometer measurement and $\mathbf{g}$ denotes the gravity acceleration vector expressed in body-fixed coordinates. The problem here considered is that of estimate the linear position of the vehicle with respect to the undisturbed position of the transponder, the linear velocity of the vehicle relative to the inertial frame, and the gravity acceleration vector, all expressed in body-fixed coordinates. This last point is of major importance in the design of Navigation Systems as, due to its magnitude, any misalignment in the estimation of the gravity acceleration vector results in severe problems in the acceleration compensation.

4.2 Proposed Solution

As in Section 3.2, let $\mathbf{e}$ denote the position of the transponder expressed in body-fixed coordinates. Its time derivative, given by (4), can be rewritten, in order to fit in the proposed design setup, as

$$\dot{\mathbf{e}} = -\mathbf{v} - \mathbf{S}\left(\boldsymbol{\omega}\right)\mathbf{e}.$$

On the other hand, from (5) it follows that

$$\dot{\mathbf{v}} = \mathbf{a} - \mathbf{g} - \mathbf{S}(\boldsymbol{\omega})\mathbf{v}.$$

Assuming the gravity acceleration vector constant in the inertial frame its time derivative in body frame coordinates can be written as

$$\dot{\mathbf{g}} = -\mathbf{S}(\boldsymbol{\omega})\mathbf{g}.$$

As in the previous example, this estimation problem falls in the class of systems (1). To be more explicit, just consider $\boldsymbol{\eta}_1 = \mathbf{e}$, $\boldsymbol{\eta}_2 = \mathbf{v}$, $\boldsymbol{\eta}_3 = \mathbf{g}$,

$$\mathbf{A}_p = \begin{bmatrix} \mathbf{0} & -\mathbf{I}_3 & \mathbf{0} \\ \mathbf{0} & \mathbf{0} & -\mathbf{I}_3 \\ \mathbf{0} & \mathbf{0} & \mathbf{0} \end{bmatrix}, \quad \mathbf{B}_p(t) = \begin{bmatrix} \mathbf{0} \\ \mathbf{I}_3 \\ \mathbf{0} \end{bmatrix},$$

and $\mathbf{u} = \mathbf{a}$. Thus, it is possible to design a Kalman filter using the technique presented in Section 2.

4.3 Simulation

To illustrate the performance of the proposed solutions the simulation presented in the previous section was modified in order to suit this new setup. The disturbances that affect the position of the buoy were kept, as well as the trajectory described by the vehicle. Gaussian noise was added to the accelerometer measurements with standard deviation of $6 \times 10^{-3}\,\mathrm{m/s}^2$.

Fig. 9 shows the singular values of the linear time invariant closed loop transfer functions from the disturbances and sensor noise to the position, vehicle velocity, and gravity acceleration estimate errors, in the inertial frame. Once again, the diagram indicates that the performance requirements are met by the filter, which is evident from the band rejection characteristics of the notch present in the figure.

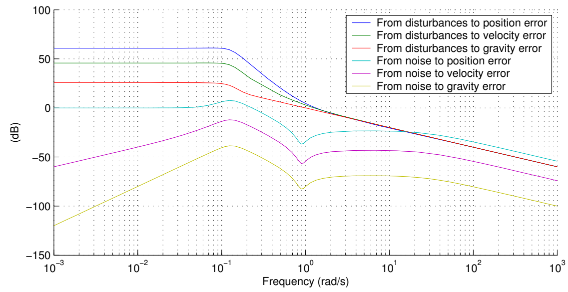

Fig. 9. Singular values of the Kalman LTI filter error dynamics

The evolution of the filter error variables is shown in Fig. 10 and, in greater detail, in Fig. 11. The results are similar to those presented in the previous section, with a slight decay in the rejection of the environmental disturbances and the noise of the sensors due to the increased order of the filter that arises from the additional effort of estimation of the acceleration of gravity.

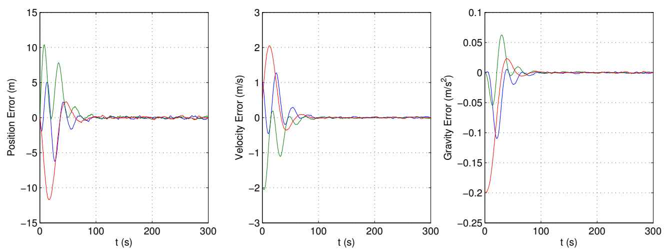

Fig. 10. Time evolution of the Kalman filter error variables

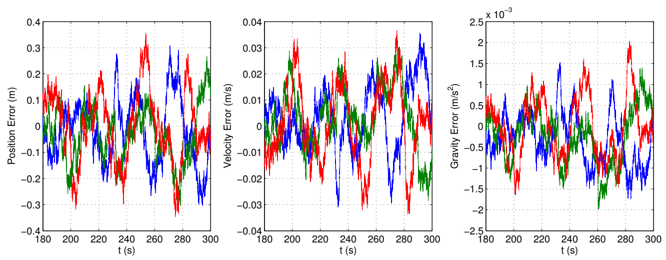

Fig. 11. Detailed evolution of the Kalman filter error variables

5. CONCLUSIONS

Navigation Systems are a key component in the design of a great variety of vehicular applications. This paper presented the design and performance evaluation of two globally stable time varying kinematic Kalman filters to estimate linear motion quantities, in three dimensions, with application to underwater vehicles. The proposed technique is based on the steady state Kalman filter for an equivalent linear time invariant system and employs frequency weights to explicitly achieve adequate wave disturbance rejection and attenuation of the noise of the sensors on the state estimates. In the first case study a Navigation filter was designed for the estimation of unknown constant ocean currents, linear position, and inertial velocity of an underwater vehicle with respect to a fixed point in the mission scenario. In the second case the proposed solution also addressed the estimation of the acceleration of gravity. The theoretical background, which applies to a broader class of systems, was briefly introduced and simulation results were offered that illustrate the filtering achievable performance in the presence of extreme environmental disturbances and realistic noise of the sensors.

Future work includes the investigation on the applicability of the proposed estimation design technique to other classes of systems. Other applications can also be devised in the design of navigation systems for other mobile platforms, like aerospace and indoor vehicles.

REFERENCES

P. Batista, C. Silvestre, and P. Oliveira. A Quaternion Sensor Based Controller for Homing of Underactuated AUVs. In *Proc. 45th IEEE Conference on Decision and Control*, pages 51–56, San Diego, USA, December 2006.

P. Batista, C. Silvestre, and P. Oliveira. Kalman and $\mathcal{H}_\infty$ Optimal Filtering for a Class of Kinematic Systems. In *Proc. 17th IFAC World Congress*, Seoul, Korea, July 2008.

H. Berghuis and H. Nijmeijer. A Passivity Approach to Controller-Observer Design for Robots. *IEEE Transactions on Robotics and Automation*, 9(6):740–754, 1993.

C. De Wit and J.-J. Slotine. Sliding observers for robot manipulators. *Automatica*, 27(5):859–864, 1991.

T. I. Fossen and J. P. Strand. Passive nonlinear observer design for ships using Lyapunov methods: full-scale experiments with a supply vessel. *Automatica*, 35(1): 3–16, January 1999.

H. Nijmeijer and T. I. Fossen (Eds). *New Directions in Nonlinear Observer Design (Lecture Notes in Control and Information Sciences)*. Springer, 1999. ISBN 978-1852331344.

R. Ortega, A. Lora, P. J. Nicklasson, and Hebertt Sira-Ramirez. *Passivity-based Control of Euler-Lagrange Systems: Mechanical, Electrical and Electromechanical Applications*. Springer, 1998. ISBN 978-1852330163.

A. Pascoal, I. Kaminer, and P. Oliveira. Navigation System Design Using Time Varying Complementary Filters. *IEEE Aerospace and Electronic Systems*, 36(4): 1099–1114, October 2000.

J.E. Refsnes, A.J. Sorensen, and K.Y Pettersen. Robust observer design for underwater vehicles. In *Proc. 2006 IEEE Conf. Control Applications*, pages 313–319, Munich, Germany, October 2006.

C. Silvestre, A. Pascoal, and A. Healey. AUV Control Under Wave Disturbances. In *Proc. of the 10th International Symposium on Unmanned Untethered Vehicle Technology*, pages 228–239, Durham, New Hampshire, USA, September 1997.

C. Silvestre, A. Aguiar, P. Oliveira, and A. Pascoal. Control of the SIRENE Underwater Shuttle: System Design and Tests at Sea. In *Proc. 17th International Conference on Offshore Mechanics and Artic Engineering (OMAE'98- Conference)*, July 1998.

R. Skjetne and H. Shim. A Systematic Nonlinear Observer Design for a Class of Euler-Lagrange Systems. In *Proc. 9th Mediterranean Conf. on Control and Automation*, Dubrovnik, Croatia, June 2001.